AADE-07-NTCE-14

Enhanced Ultrasonic Measurements for Cement and Casing Evaluation

C. Morris, Schlumberger, J. Vaeth, Schlumberger, R. van Kuijk, Schlumberger, B. Froelich, Schlumberger

Abstract

Zonal isolation prevents the production of fluids from non-completion intervals, contamination of ground water by fluids in the wellbore, and allows conformance control of injected fluids. Current acoustic evaluation techniques may be limited by the acoustic properties of the material behind casing and by the inability to see beyond the cemented region near the casing. A new ultrasonic imaging tool has been developed to address these limitations.

The new imager tool combines the classical pulse-echo technique with a new ultrasonic technique that provides time-based echoes arising from propagation along the casing and also reflections at the cement-formation interface. Processing these signals yields unprecedented characterization of the cased-hole environment in terms of the acoustic velocity of the material immediately behind casing, the position of the casing within the borehole, and the geometrical shape of the borehole.[4]

In order to provide answers to the casing/cement evaluation questions, a field study was performed to evaluate the results provided by both sonic tools and this new ultrasonic tool in the different cement materials, drilling fluids, and casing sizes. Examples are presented to illustrate the actual response of the ultrasonic tool to these various completion environments including wells cemented with conventional and lightweight cement. The results demonstrate enhanced cement evaluation for all cement types and a significant reduction in the uncertainty in making a squeeze or no-squeeze decision. The new cement evaluation tool implements both the traditional pulse-echo technique and the new flexural wave concept. The flexural mode enables deep imaging of the cement sheath up to the cement-formation interface. In addition, the measurement of the borehole geometrical shape makes it possible to evaluate double casing string conditions for potential damage.

Introduction

Sonic logging tools have been used since the 1960's to evaluate the placement of cement for hydraulic isolation of formations. There have been several advancements in the logging tools that improved the ability to evaluate the cement sheath since that time. During the same period of time there had been little change in the types of cement. In the past few years, however, there has been an emphasis on optimizing the cementing operation and reducing the overall cost of the completion. To the initial cementing operation, this meant developing lightweight and specialized cements that would allow setting casing strings deeper without worrying about lost returns. Other gains in efficiency were also achieved using lighter cements while drilling and completing weak formations. Changes in these new cements, and their acoustic properties, have also brought about the need for re-evaluating the techniques and tools used for the evaluation of these cements with the sonic logging tools currently available.

Perhaps the most significant development in cement evaluation technology was the ultrasonic logging tools. The ultrasonic type tools are designed to measure the acoustic impedance of the material on the outer surface of the casing. This is accomplished by using a transducer to project a short pulse of acoustic energy with a bandwidth of 200 kHz to 700 kHz toward the casing.[1] The transducer emits high frequency ultrasonic pulses that travel through the liquid and into the casing wall, resonating the casing in the thickness mode. The transducer then becomes a receiver and measures the returning echo from the casing. The returning waveform is the summation of the echo waveform from the original burst, and an exponentially decaying waveform from the resonant energy trapped between the inner and outer casing walls. The analysis of the returning wave can be performed in several different ways with the outputs being acoustic impedance of the material on the outside surface of the casing and thickness of the casing. Current versions of the ultrasonic tools have a rotating transducer that provides full radial coverage of the casing circumference. These tools have far better vertical and radial resolution than the CBL type tools.[1,2,3]

The interpretation of the zone isolation for the ultrasonic tools is determined by the selection of a liquid/cement threshold for acoustic impedance. Where the acoustic impedance is greater than the liquid/cement threshold, the casing is interpreted as cemented. Where the acoustic impedance is less than the liquid/cement threshold, the casing annulus material is interpreted to be fluid. An image of the acoustic impedance measurements and an image of the interpreted data can then be created to provide a visualization of the cement in place. The key parameter for the interpretation of the ultrasonic tools is the selection of the liquid/cement threshold, which is based on the acoustic impedance of the liquids that could be outside the casing, rather than the cement that might be in contact with the casing. Therefore, it is not really necessary to know the acoustic

properties of the cement in great detail when logging with ultrasonic tools. There are statistical approaches used to enhance the interpretation of ultrasonic logs where gas-contaminated cement, gas-filled microannulus, or liquid-filled microannulus is present[2].

The ultrasonic tools have two main advantages over the basic sonic cement evaluation tools. First, the ultrasonic logging tools are capable of much better vertical and radial resolution. This provides the interpreter an improved "picture" of what the cement sheath looks like. Second, the interpretation of the cement is not dependant on the specific acoustic properties of the cement. The ultrasonic interpretation is sensitive to the acoustic properties of the fluids. The only requirement is there must be at least a 0.5 MRayl difference between the acoustic impedance of the fluid and the acoustic impedance of the cement. This is considered to be the accuracy of the acoustic impedance measurement.

The new Isolation Scanner* ultrasonic cement evaluation tool (the rotating sub is illustrated in **Fig. 1**) is based on a combination of the thickness resonance mode, described above, and a second flexural mode described by Kuijk et al.[4] It makes use of four transducers located in a rotating sub. One is the normal incidence transducer; the others are a flexural wave transmitter and two receivers, with the flexural wave propagating vertically along the casing.

The radiation of the pulse into the inner and outer media, with respect to the casing, is accompanied by attenuation of the flexural wave amplitude along its path. This flexural attenuation is computed from the amplitude ratio of the casing arrivals on the near and far flexural receivers. It is sensitive to the mechanical properties of both inner and outer materials and is approximately the sum of the attenuation due to the inner fluid and the outer material. The flexural transducers are operating at about 200 kHz, and their azimuthal resolution is similar to the pulse-echo transducer (30 mm). Both the cement impedance from the normal incidence transducer and the flexural attenuation are used to quantify the annular material in contact with the casing as solid, liquid, or gas.

The pulse radiated into the annular space may be reflected by the third interface, the cement/formation surface (the inner and outer casing walls being the first and second interfaces seen by the ultrasonic signal) if there is sufficient acoustic contrast between the annular and formation material. As the flexural wave propagates along the casing, with a group velocity independent of frequency, the casing arrivals are compact in time and any echo that is late in the wave train is therefore easily visible and detectable. This makes it possible to accurately measure the time of arrival and amplitude of the Third Interface Echo (TIE). The TIE contains information about the annulus material properties and the formation wall geometry. Factors affecting the TIE include: casing eccentering, signal attenuation in the annulus material, acoustic contrast between the annulus material and formation, surface roughness, and signal travel distance.

* Mark of Schlumberger

Discussion of Results

Field tests, three of which are presented below, were performed in different fluid environments and with different casing/cement sheath material, including new lightweight cements, to determine the practical operating limits of ultrasonic tools. The acoustic attenuation response of the tool was investigated in both oil-base and water-base drilling mud systems.

Example 1:

During production through 5-1/2" production tubing inside 9-7/8" casing that is inside 13-3/8" (and 13-5/8") outer casing, this well showed a pressure increase on the backside of the production tubing (A-annulus). Flow behind casing diagnosis revealed the possibility of a leak into the 9-7/8" annulus (B-annulus). It was decided to pull the completion string to evaluate the cause of the pressure increase. The completion string was cut above the packer but could not be pulled. Free point and stuck pipe logs were run in the 5-1/2" production tubing to identify why the tubing would not pull free. These logs showed that there was damage to the 5-1/2" tubing and that it was pinched across the interval from 14880–14810 ft, as seen in **Fig. 2**. To determine the condition of the 9-7/8" or the 13-3/8" (and 13-5/8") outer casing above the stuck point, it was decided to pull the free portion of the 5-1/2" tubing and run the Isolation Scanner tool in the 9-7/8" casing from 14700 to 9700 ft.

Reflections from the inner and outer casing were tracked continuously and show no damage or deformations. The deviation is ~35 deg throughout most of the interval. The inner casing is resting on the bottom side of the outer casing for most of the logged interval. The annular space between the two casing strings is filled with a liquid. The inner casing size is 9-7/8", 62.8 lbm/ft (with a thickness of 0.625") filled with presumably 11.6 lbm/gal CaCl / CaBr. The annulus is filled with brine, presumably 11.1 lbm/gal CaCl brine.

The integrated results for these mud parameters are very consistent along the full log interval at about 2.95 MRayls and 172 μs/ft for acoustic impedance and slowness, respectively. The 11.6 lbm/gal brine would be expected to have a theoretical acoustic impedance of about 2.6 MRayls and this value was used for the standard pulse-echo processing.

Fig. 3 shows the BATT (attenuation) curve and the VDL from the CBL type tool, the SLG map, and flexural waveform VDL across two perpendicular diameters. As expected, the SLG map is mostly liquid, with some indication of solid material at bottom and top. The flexural VDL (not aligned with the relative bearing) displays consistent TIE from the 13-3/8" outer casing. From bottom to ~12500 ft, the TIE at azimuth 90 deg merges with the 9-7/8" casing arrival, and cannot be visually separated from it. Because of this contact between the two casings, the TIE detection on the near side is somewhat noisy.

Fig. 4 shows the following tracks: the SLG map from Isolation Scanner (computed from pulse-echo and flexural mode measurements), the flexural attenuation, the annulus acoustic impedance (AIBK), the amplitude ratio between the

TIE and the casing arrival, the TIE time of arrival, the annulus thickness computed from the TIE time of arrival and an assumed slowness of 172 μs/ft for the fluid inside the annulus, and a curve giving the maximum annulus thickness. All maps are oriented with the relative bearing, with top of the hole at center of the image (This is opposite to the usual display convention where bottom of the hole is at center of the image). The amplitude ratio map shows a bright line which corresponds to the wide side of the annulus. As expected, this wide side is usually located at the high side (top) of the hole, except, for example, in the zone 10600-10400 ft, where the wide side is at the low side (bottom) of the hole. Such a configuration is due to the 9-7/8" casing buckling inside the 13-3/8"or a change in the hole shape, with a local kink on the deviation curve from 11000-10000 ft. The narrow side of the annulus generates galaxy patterns both on the acoustic impedance map and the flexural attenuation map.

On the TIE amplitude map, there is a change in brightness of the central line at a depth of 11652 ft which seems to correspond to the change in outer casing (from 13-3/8" to 13-5/8"). It should be noted that both casings should have the very similar internal diameter (12.346" for the 13-3/8" and 12.38" for the 13-5/8"), and thus cannot be distinguished on the transit time map. The change of casing is also apparent on the flexural VDL, with longer TIE in the top part than on the bottom part.

Apart from the location of the wide side, both amplitude and transit time maps are very consistent from top to bottom with no indication of deformation of the outer casing. The last track to the right gives the maximum annulus thickness and its value is close to 60 mm (assuming a fluid slowness of 172 μs/ft), for an expected value of 63 mm. A few locations exhibit a smaller value (e.g. 13100 ft) when the two casings are not in contact.

Below 14500 ft, the amplitude map displays lower values on the side of the casing. Such lower amplitudes induce some occasional miss picks of the TIE, and can also be correlated with indications of solid material on the SLG map. It seems likely that some attenuating deposits are present at these locations.

Fig. 5 shows an upper section of the well where the 9-7/8" casing is not centralized inside the 13-5/8" casing. The polar plots show graphically the relative casing positions with depth.

Example 2:

The Isolation Scanner tool was run, in combination with neutron porosity and dipole sonic tools, eight days after the cementing job with the logging fluid being a 3% KCL brine. During the cementing operations, intermittent flow pack-off was observed during the final 50 Bbl displacement. During log acquisition in the 7", 23 lbm/ft casing, vertical sampling was set at 3" and the azimuthal sampling at 10 deg. The pulse-echo technique was processed with a mud impedance value of 1.68 MRayls and a fluid velocity of 203 μs/ft. The cement evaluation logs were run with the wellbore under 1000 psi pressure.

The full log is displayed in **Fig. 6**, and shows homogeneous lightweight cement from bottom to 4250 ft, with an acoustic impedance of around 4.0 MRayls. Within this section, some intervals like 5400-5200 ft display poorer cement with patches of liquid or even gas behind the pipe. The top section 4250-3900 ft is a succession of free pipe and poorly cemented zones.

Occasionally over the log, the TIE is strong enough to trigger the recording window, instead of the casing arrival. This occurs whenever the TIE amplitude is more that three times stronger than the casing arrival. These events usually produce a white dot on the SLG map (unknown state of material), as for collars/centralizers. **Fig. 7** details a section with very homogeneous cement from 6650 to 6400 ft. The top part exhibits some patches of liquid and gas. The gas indication is coming from the low acoustic impedance and low flexural attenuation. Moreover, the VDL at the corresponding depths shows a high frequency ringing following the casing arrival. Such ringing is due to parasitic extensional mode signals with low attenuation where the casing is in contact with gas on one side. Another gas spot is shown on **Fig. 8**, where it is clear on the VDL across the gas zone that both extensional and TIE are superimposed. This is a clear indication that cement is present in the annulus, allowing propagation to the formation wall, but this cement is debonded from the casing, with a dry microannulus separating them. The cement is connected to the casing through occasional contact points, allowing some transmission of the acoustic pulse in the cement, while the flexural attenuation and acoustic impedance measurements see mostly gas.

Fig. 7 track 5 displays the TIE ratio amplitude map which shows formation bedding, some very thin, as can be checked on the VDL track. Because the TIE is often very weak, these transit time picks and the estimated cement velocities are not reliable, except in the central zone 6480-6460 ft. The apparent cement velocity is around 1500 m/s, but most probably the picked arrival is a mixed compressional/shear arrival, and the computed velocity is therefore an average of cement compressional and shear velocities.

Fig. 9 is a polar plot at 5225 ft, where at least two clear sets of TIE are visible. The inner (faster) echo can be identified most probably as a compressional arrival, the next one as a shear. The TIE have been fitted with circles and the apparent velocities extracted from the diameters are the compressional velocity (Vp) of 2250 m/s, and a mixed compressional/shear velocity of 1500 m/s, assuming a 8.5" borehole. The shear velocity Vs computed from these two values is Vs = 1090 m/s. From the acoustic impedance = density ∗ Vp = 4 MRayls, one can derive the cement density at ~14.8 lbm/gal. The casing centering at this depth is 64% from the distance of the fitted circles center to the casing arrival center.

Fig. 10 is for another section with far more TIE picks, so that the cement velocity and casing centering (black curve in track 6) are reliably computed in the top interval 5420-5350 ft. The casing centering is ~80%, as can be expected for an in gauge vertical well, with one centralizer every 3 casing joints. The cement top section is displayed on **Fig. 11**. Above 4250

ft, alternating zones of free pipe and poor cement are present. The TIE amplitude image is strongly correlated with the SLG map, with strong amplitudes in free pipe. However, it also seems to correlate with the GR (see the bed at 4140 ft), so that a lithology effect on the cement cannot be excluded. The annulus velocity, as measured in the free pipe zones, is ~1500 m/s, as can be expected for water. The casing is again rather well centralized at ~80%. At a depth of ~4280 ft, below the cement top, the annulus compressional velocity is reliably estimated at ~1800 m/s (orange band on track 6). This rather low value compared to the expected value of standard cement (~3000 m/s) is explained by contamination likely to occur close to the cement top.

Example 3:

Operators have an enormous investment in their deepwater platforms in the Gulf of Mexico; thus, re-completions and sidetracks are necessary to ensure effective reservoir depletion and consistent hydrocarbon flow. There are a limited number of wells that can be drilled and produced from one platform, which is dictated by the sea floor template slots. In order to fully utilize all slots, the non-cemented intermediate and production casing strings from existing wells must be retrieved in order to begin new drilling projects, drill sidetracks, or perform re-completions. On many attempts at casing retrieval, problems are encountered. To increase the cut and pull operational efficiency, drilling engineers need to accurately determine the entire completion environment of multiple cemented and non-cemented concentric casing strings.

The drilling fluid effect commonly known as "barite sag" effectively cements the pipe in place. Mud sag occurs when the original drilling fluid in the non-cemented annulus degrades over time with the solids settling to the lower portion of the hole, or to changes in deviation (doglegs). It was found that accurate ultrasonic measurements could be used to differentiate between cement, mud solids, liquid, and gas. This unique technology can directly measure the acoustic velocity of the annular space material as illustrated in the previous examples.

The settled solids, most commonly barite, greatly increase the friction forces acting on the exterior of the casing. For example, consider a 7" casing interval with mud sag in the annulus. If the mud solids add 25 psi additional friction force (experimental data suggests it is closer to 50 psi) to the recovery operation, it would require an additional 6600 lbf/ft to pull the casing. With this increase, the force needed to pull the casing could quickly exceed the capacity of the drilling rig.

In addition, it is important to identify casing wear or other casing anomalies as they can significantly impact the mechanical integrity of the casing during the cut and pull operation. One critical factor to identify is casing "touch points" where the casing is in contact with either the outside casing or the formation. This contact can also increase the friction acting on the outside of the casing, increasing the force necessary to pull the casing.

The Isolation Scanner tool was run in combination with a sonic type tool on this well with 7", 38 lbm/ft casing inside 9-5/8", 43.5 lbm/ft outer string. The logged interval from x300-x000 ft is shown in **Fig. 12**. The borehole fluid was brine of 8.6 lbm/gal density. For the acquisition, the vertical sampling was set at 3", and the azimuthal sampling at 5 deg. The pulse-echo technique was processed with a mud acoustic impedance value of 2.03 MRayls. The results show that the lower zone annulus was generally cemented. Third interface reflections were mostly present in the cemented zone and in the double casing string (9-5/8" outer casing). The results show the 7" casing was poorly centralized, even where mechanical centralizers are present on each joint, and touching the outer casing.

The interval shown from x300-x000 ft shows a high impedance annular space that is consistent with Class G cement and/or highly packed mud solids. The 7" casing is in almost continuous contact with the 9-5/8" casing on the 180 deg side. This is verified by the galaxy patterns seen in the cement map image. There is little cement at the touch points, but almost complete coverage otherwise. The measured impedance is greater than 6.5 MRayls over this interval, which is equivalent to 3500+ psi compressive strength cement.

In addition, measurements were used to determine the material (cement, mud solids, liquid, or gas) in the annulus to evaluate potential casing pulling operation risks for upper intervals. **Fig. 13** shows results through an upper interval with a change in wellbore deviation. There is significant mud sag across this 'free pipe' zone. From these images, the contact area can be calculated and the potential pulling force estimated.

The 9-5/8" casing also appears to be very deformed or corkscrewed over a shallower interval, as can be seen in **Fig. 14** showing the third interface VDL. The casing and annular material results can also be visualized in 3D images as shown in **Fig. 15**.

Conclusions

The new cement imaging tool implements both the traditional pulse-echo technique and the new flexural wave concept. This combination is more precise and reduces the uncertainty in evaluating the material immediately behind casing further than either of the two techniques alone. This improves the interpretation of zone isolation even in lightweight cements. The processed measurements are displayed in easily interpreted formats as a cement map or a channel map. It provides an enhanced resolution of the contrast between the cement and the displaced mud.

In addition, the reflections from the formation or third interface may be detected. They enable the imaging of the cement sheath up to the cement-formation interface as never before and provide information about the casing position in the borehole, an estimation of the borehole shape, or an estimation of the velocity of sound in the cement.

Accurate ultrasonic measurements make it possible to identify cement, mud solids, liquid, and gas behind the casing. For more efficient casing pulling operations, the drilling mud sag (solids) conditions can be determined in the annular space between casing strings as well as relative casing positions.

Nomenclature

AI = *Acoustic impedance*
AIBK = *Acoustic impedance map*
BATT = *Sonic tool attenuation*
BI = *Bond Index*
DATN = *Sonic tool attenuation*
Flex Attn = *Flexural wave attenuation*
SLG = *Solid, Liquid, Gas*
TIE = *Third Interface Echo*
VDL = *Variable Density Log*

References

1. Hayman, A.J., Hutin, R., and Wright, P.V.: "High-Resolution Cementation and Corrosion Imaging By Ultrasound", paper KK, SPWLA 32nd Annual Logging Symposium, June 16-19, 1991.
2. Butsch, R.J.: "Overcoming Interpretation Problems of Gas-Contaminated Cement Using Ultrasonic Cement Logs," SPE paper 30509, SPE Annual Technical Conference and Exhibition, Dallas, TX, October 22-25, 1995.
3. "Cement Sheath Evaluation," American Petroleum Institute, Technical Report 10TR1, First Edition, June 1996.
4. Kuijk, R. van, Zeroug S., Froelich, B., Allouche, M., Bose, S., Miller, D., le Calvez, J.-L., Schoepf, V., Pagnin, A.: "A Novel Ultrasonic Cased-Hole Imager for Enhanced Cement Evaluation, IPTC paper 10546 presented at the International Petroleum Technolgy Conference, Doha, Qatar, 21-23 November 2005.

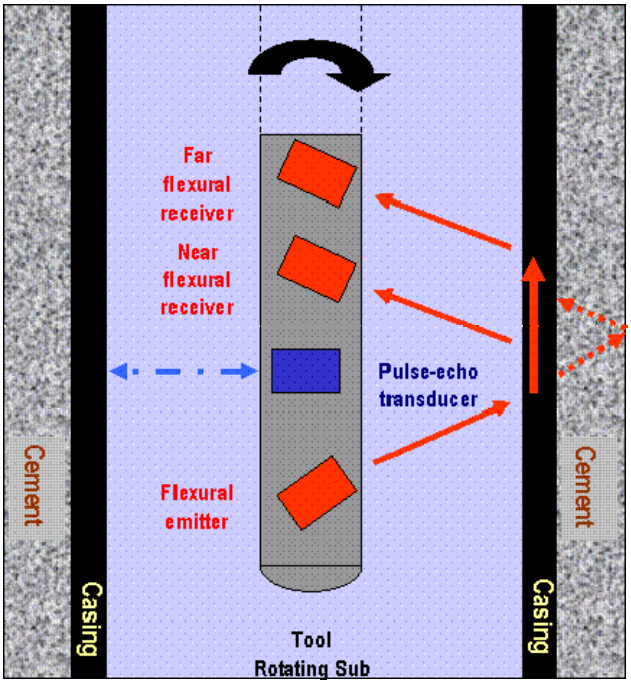

Fig. 1 – Sketch of the four transducers in the Isolation Scanner tool (rotating sub assembly).

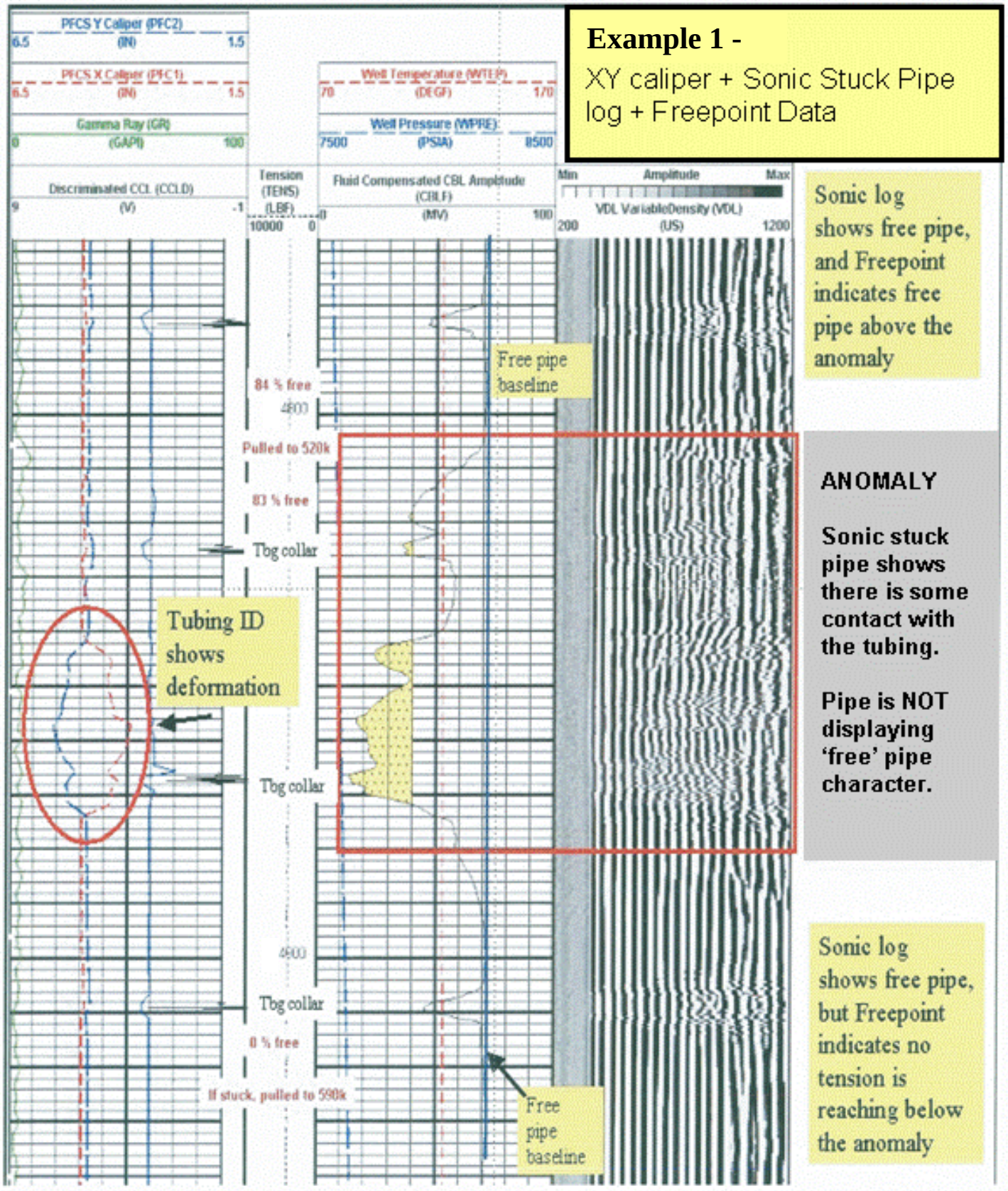

Fig. 2 – Stuck pipe logs run in 5-1/2" production tubing from 14880-14540 ft.

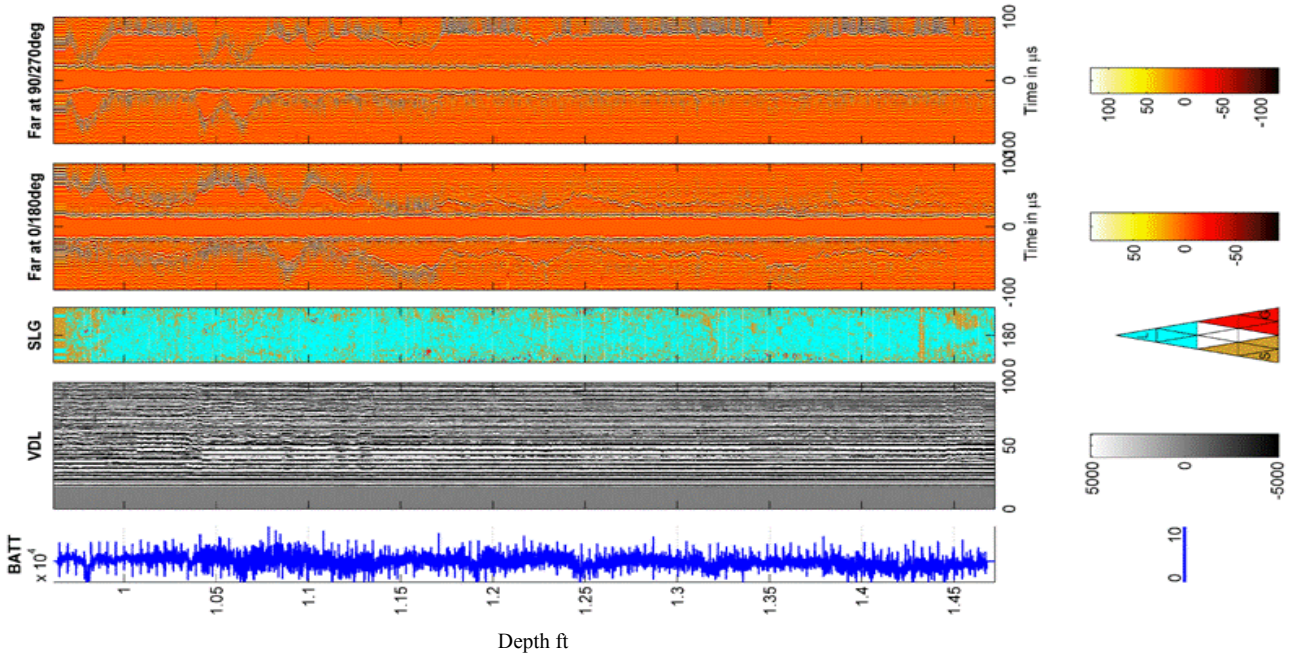

Fig. 3 – Full logged interval from 14700-9700 ft with VDL, SLG map, and flexural waveforms along two diameters.

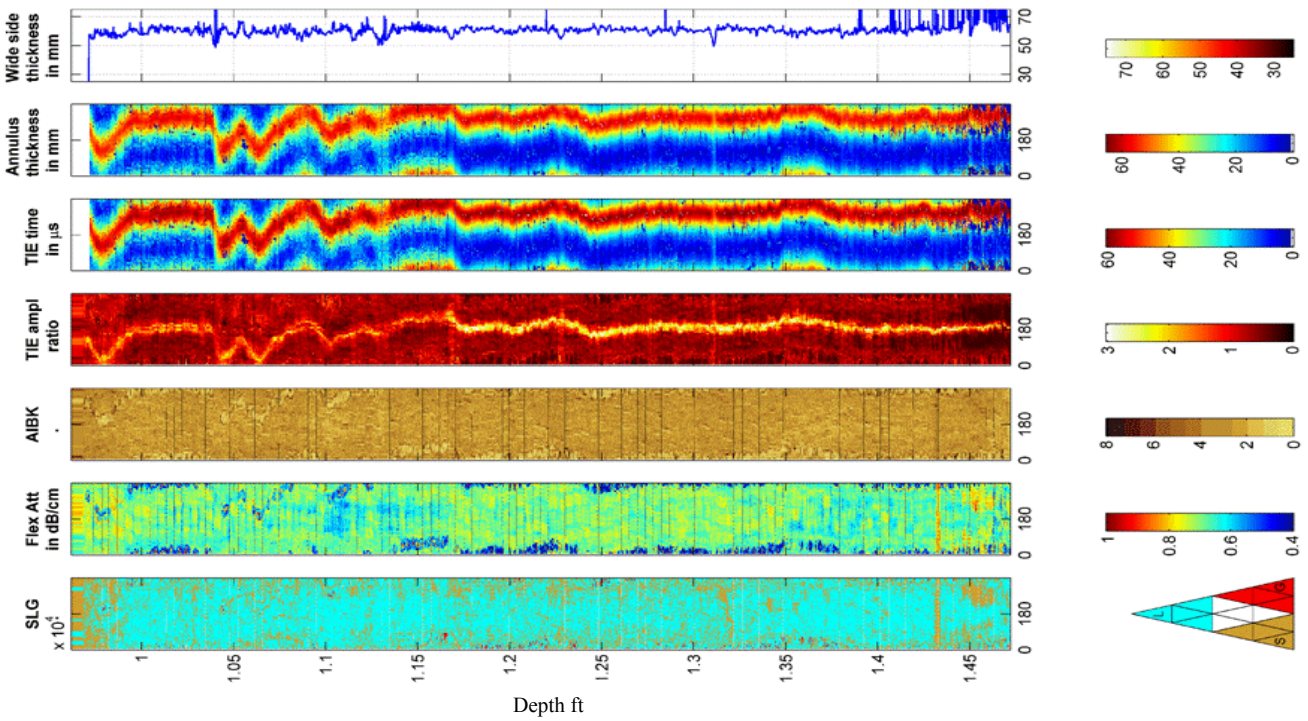

Fig. 4 – Full logged interval from 14700-9700 ft with SLG map, flexural attenuation, acoustic impedance, TIE/casing ratio, annulus transit times, annulus thickness, and maximum annulus thickness.

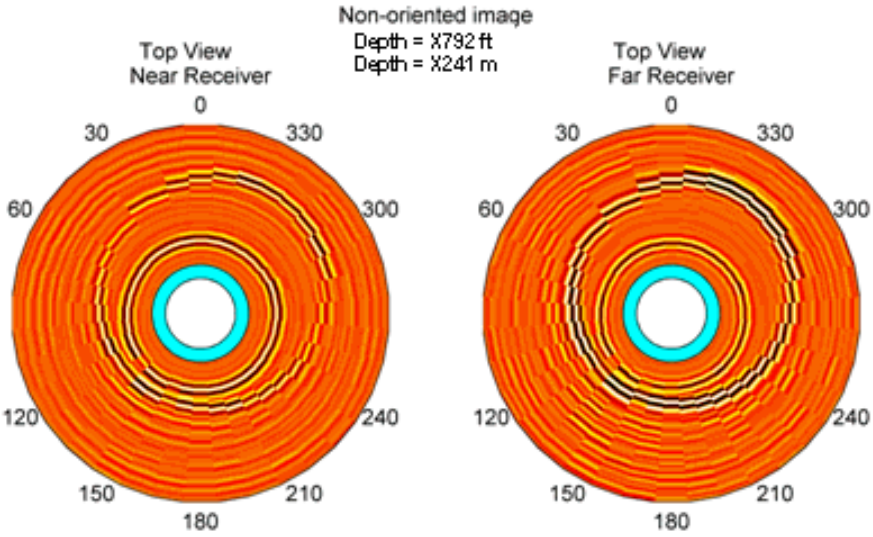

Fig. 5 – Upper wellbore section with two casing strings showing relative position of the casing within the borehole using the TIE measurements. The SLG map and zone isolation images are also illustrated at each depth cross section.

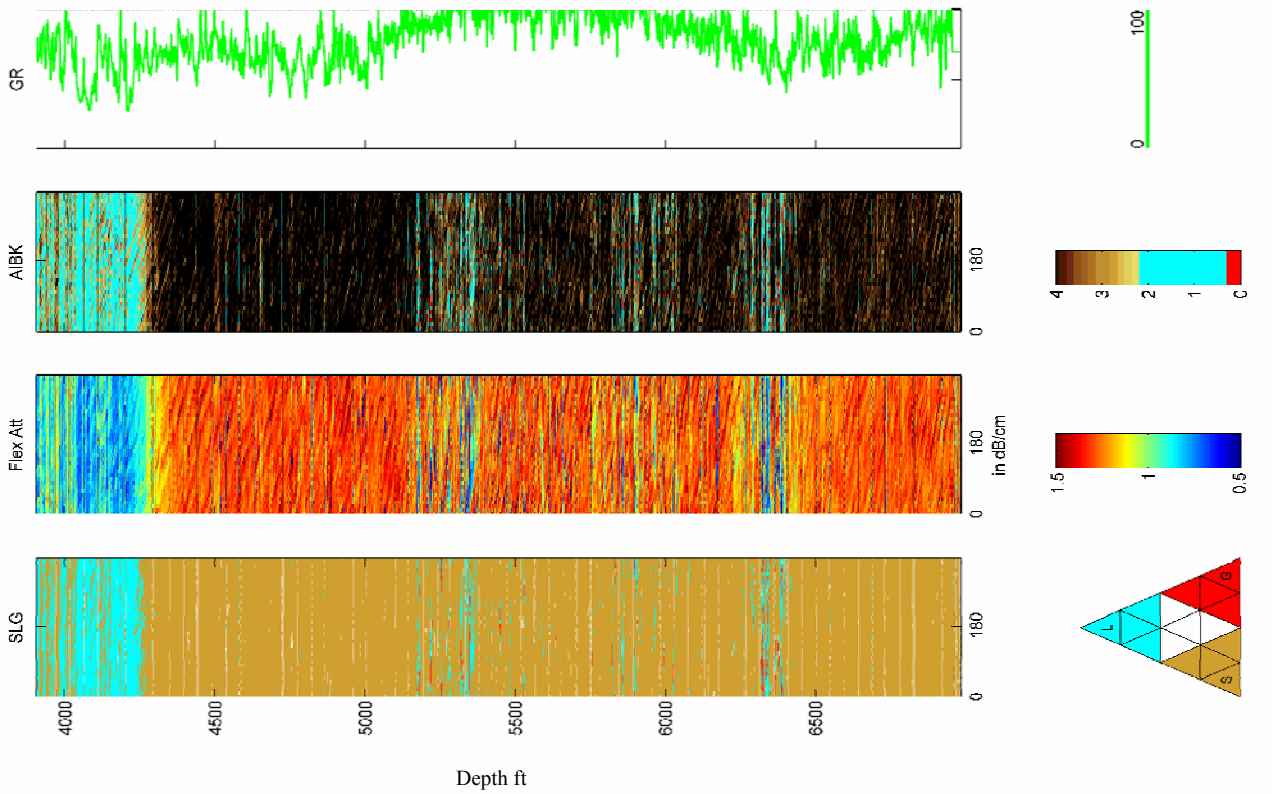

Fig. 6 – Complete log with SLG map, flexural attenuation, acoustic impedance map, and Gamma Ray curve.

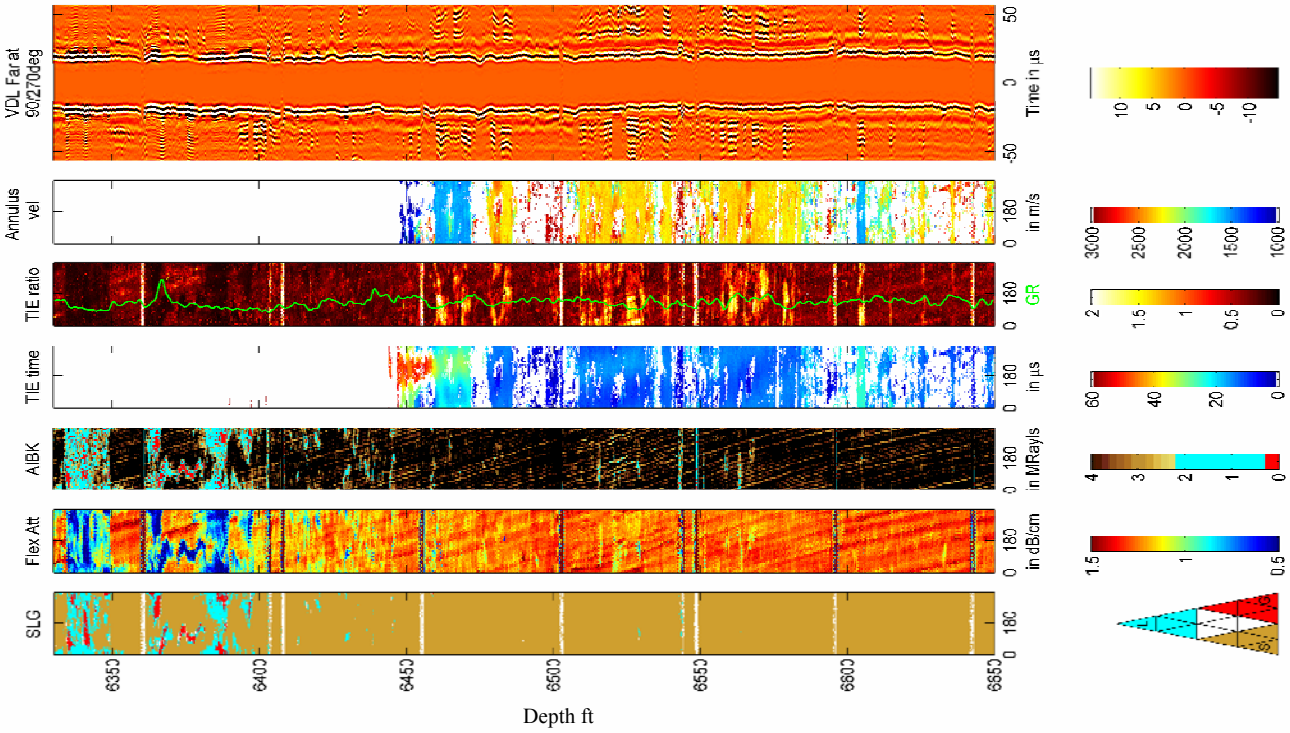

Fig. 7 – Both good and poor zone isolation shown in interval with SLG map, flexural attenuation, acoustic impedance, TIE time, TIE ratio (with GR), annulus velocity, and VDL of Far receiver waveforms across diameter azimuth 90-270 deg.

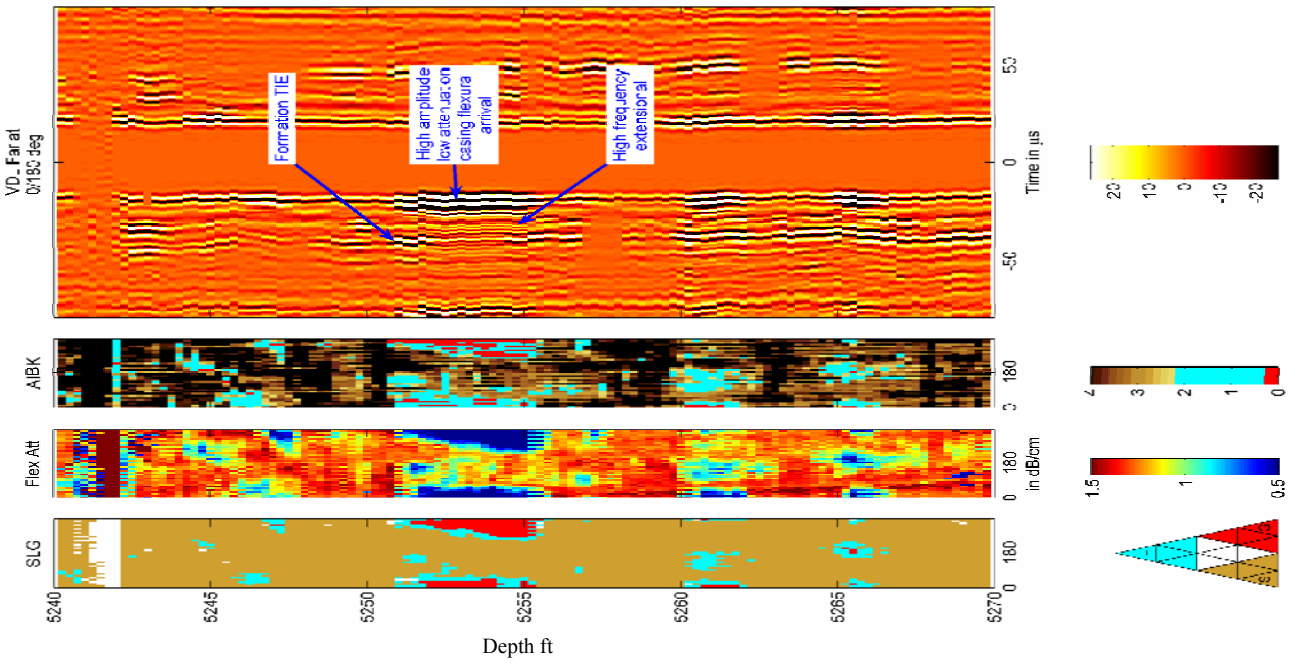

Fig. 8 – SLG map, flexural attenuation, acoustic impedance map, VDL of Far receiver waveforms in the 0-180 deg direction across the dry microannulus at 5255-5254 ft.

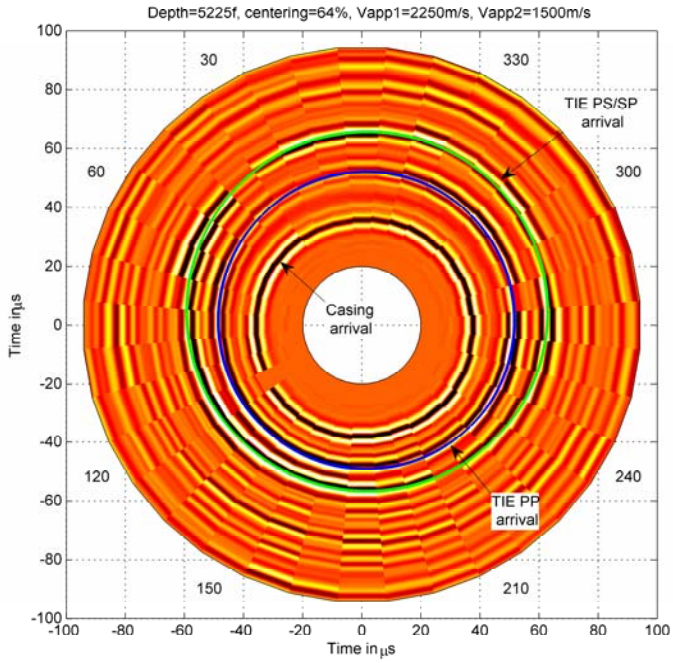

Fig. 9 – Polar plot of Far receiver with circles fitted over the compressional/shear arrival (blue) and shear arrival (green). The casing is centered about 64%.

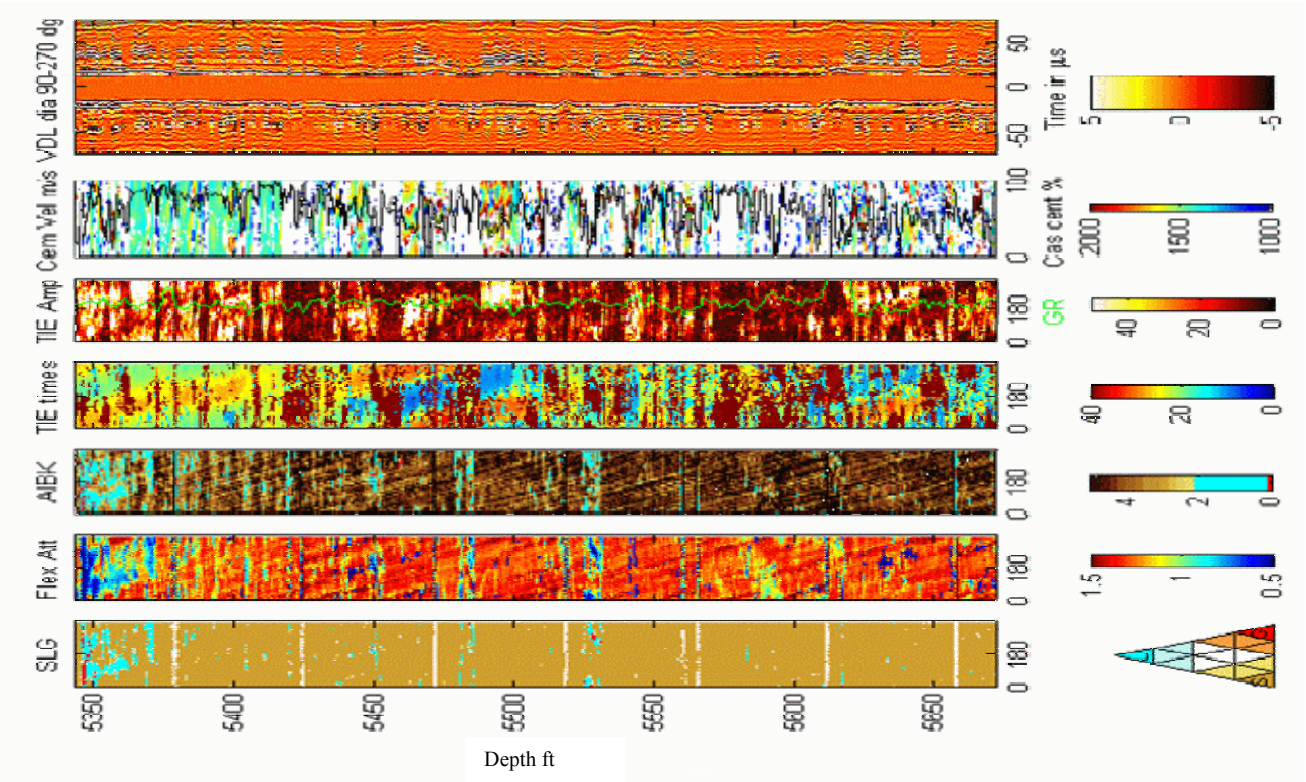

Fig. 10 – Cemented section with SLG map, flexural attenuation, acoustic impedance, TIE times, TIE amplitudes (with GR), cement velocity map (with casing centered in %), and VDL of Far receiver waveforms across diameter azimuth 90-270 deg.

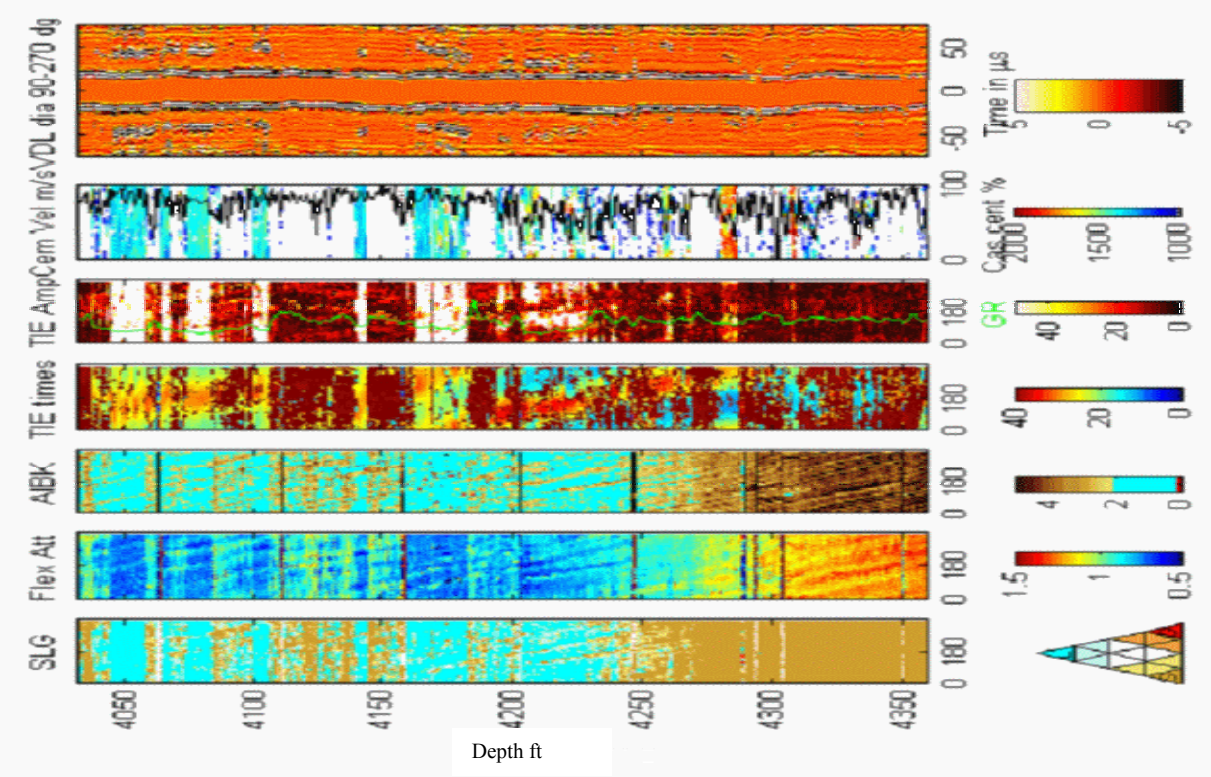

Fig. 11 – Cement top section showing SLG map, flexural attenuation, acoustic impedance, TIE times, TIE amplitudes (with GR), cement velocity map (with casing centered in %), and VDL of Far receiver waveforms across diameter azimuth 90-270 deg.

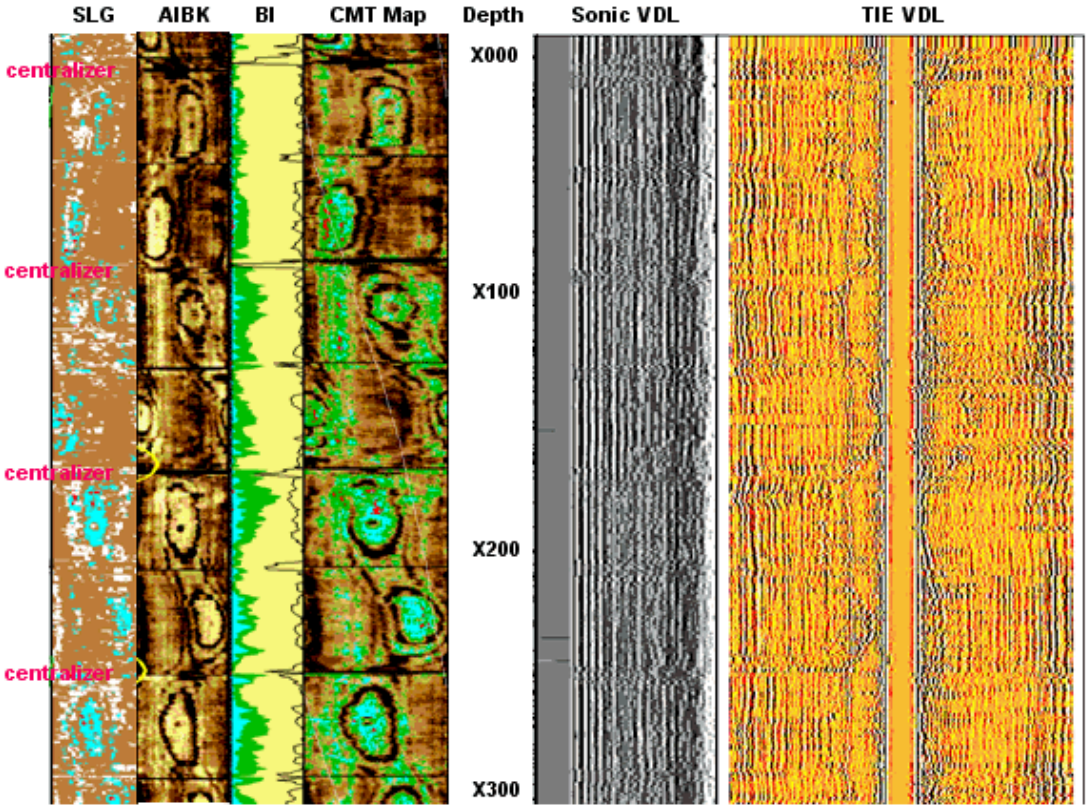

Fig. 12 – Zone of interest shown with SLG map, acoustic impedance, bond index, cement map, sonic VDL, VDL of Far receiver waveforms across diameter azimuth 90-270 deg.

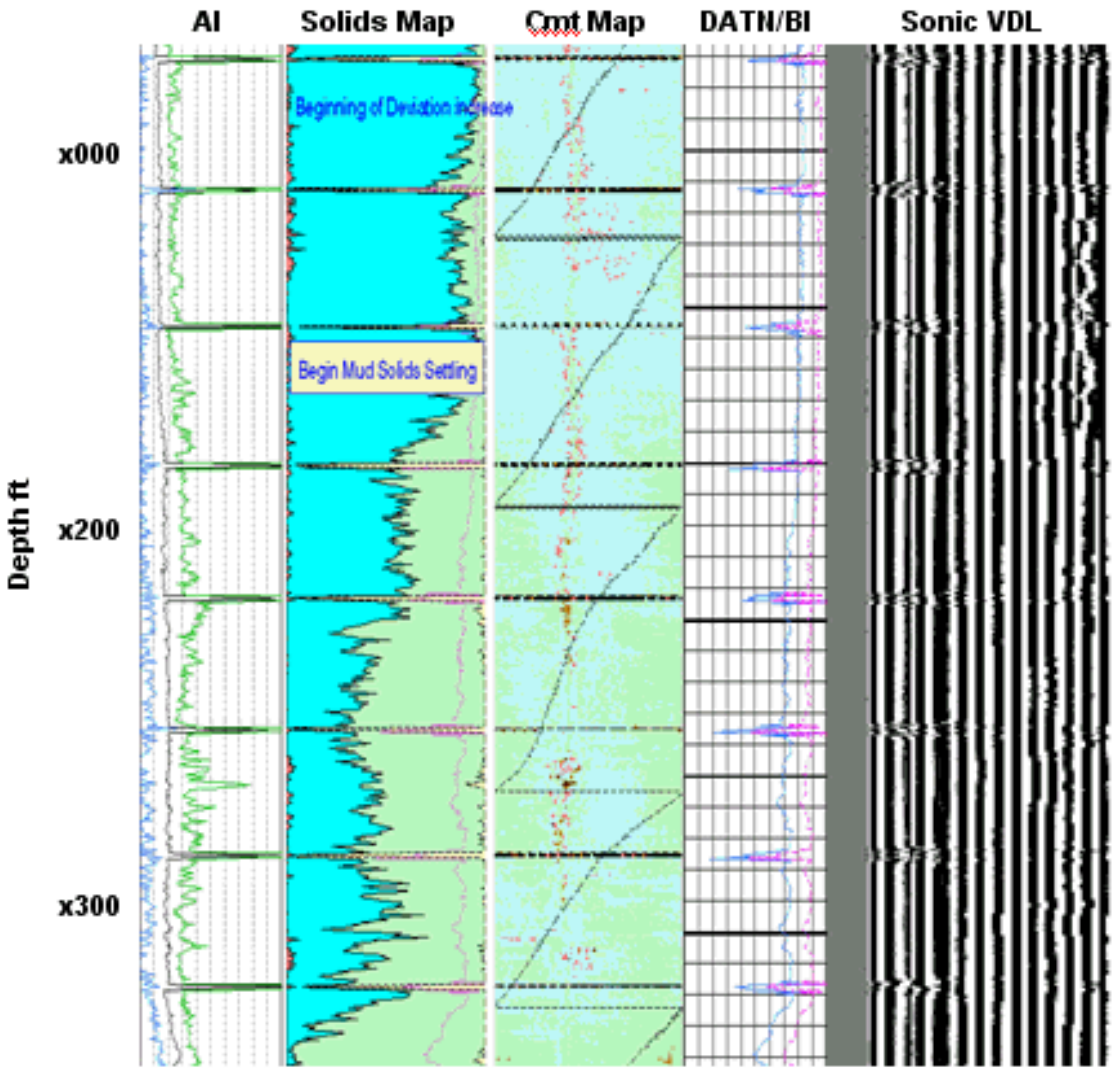

Fig. 13 – Mud sag in upper interval through a wellbore deviation interval.

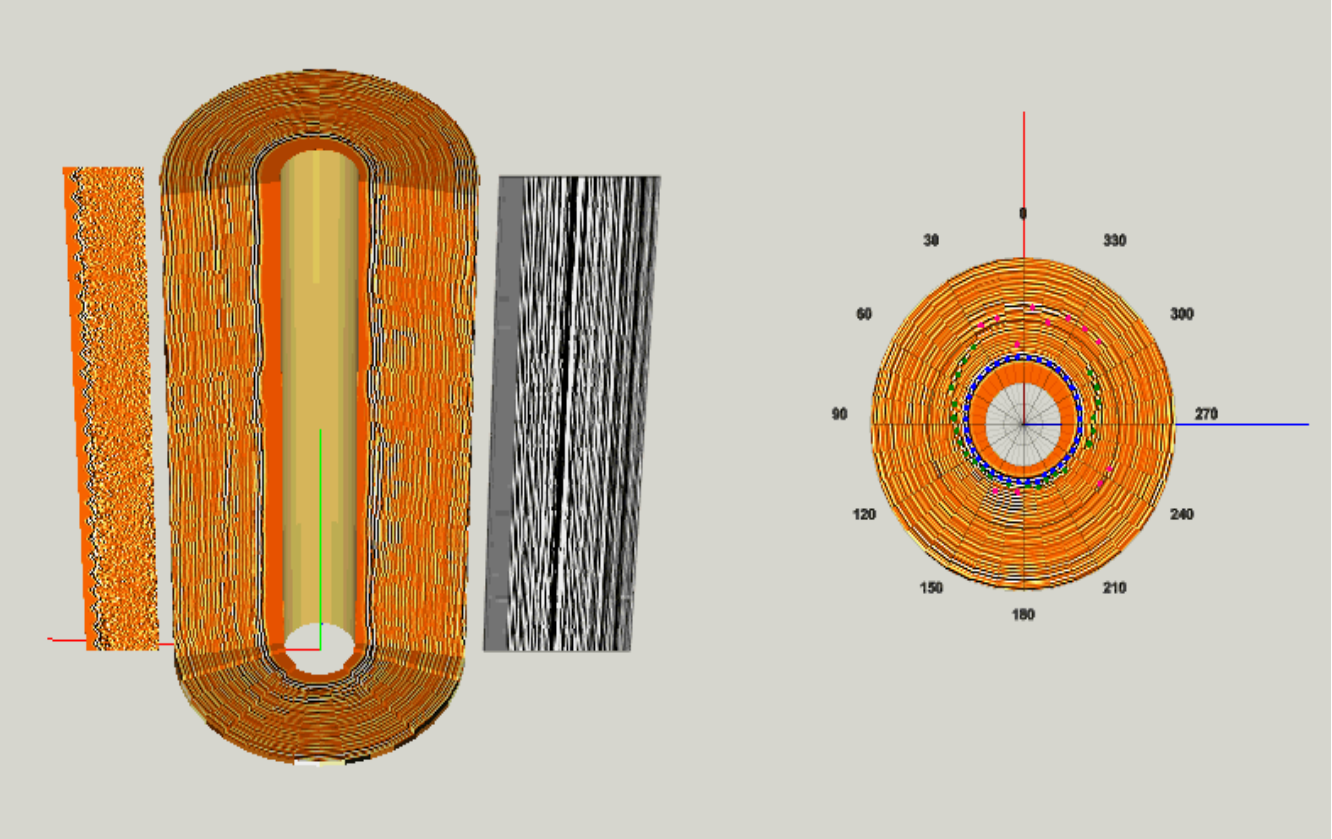

Fig. 14 – 3D images of the flexural waveforms. The first echoes from the center are the 7" inner casing arrivals, while the following ones are TIE reflections from the outer 9-5/8" casing. Fainter echoes after the first TIE are multiple reflections (up to 5) within the annulus. Such a display provides a geometrical sketch of the casing strings, where contact points or potential defect can be located.

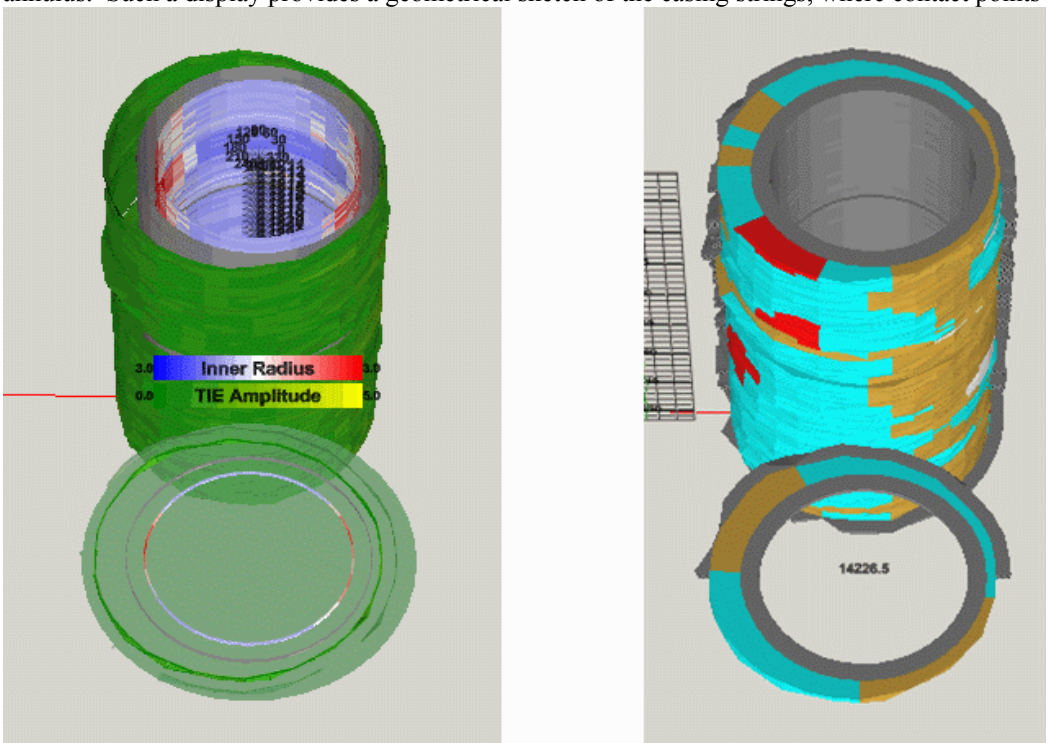

Fig. 15 – 3D images of the casing dimensions, geometric shape, and annulus materials are displayed over the shallow interval with poor cement isolation.